arXiv:0809.3776v1 [cond-mat.soft] 22 Sep 2008

Charge Renormalization, Effective Interactions, and Thermodynamics of Deionized Colloidal Suspensions

A. R. Denton†

Dept. of Physics, North Dakota State University, Fargo, ND, U.S.A. 58108-6050

Abstract. Thermodynamic properties of charge-stabilised colloidal suspensions depend sensitively on the effective charge of the macroions, which can be substantially lower than the bare charge in the case of strong counterion-macroion association. A theory of charge renormalization is proposed, combining an effective one-component model of charged colloids with a thermal criterion for distinguishing between free and associated counterions. The theory predicts, with minimal computational effort, osmotic pressures of deionized suspensions of highly charged colloids in close agreement with large-scale simulations of the primitive model.

PACS numbers: 82.70.Dd, 83.70.Hq, 05.20.Jj, 05.70.-a

† Electronic address: alan.denton@ndsu.edu

1. Introduction

Colloidal suspensions of charged macroions — nanometers to micrometers in size and dispersed in a fluid by Brownian motion — are ubiquitous in nature and industry [1, 2]. The remarkable thermal, optical, and dynamical properties of colloidal materials hinge on a delicate balance between competing interparticle interactions [3]. Common examples include aqueous paints, detergents, and clays: dispersions of latex particles, ionic surfactant micelles, and mineral platelets, respectively. Self-assembled crystals of synthetic, monodisperse, silica or polystyrene microspheres provide useful scaled-up models of atomic crystals and promise novel technologies, such as photonic band-gap materials [4, 5]. As predicted by the classic theory of Derjaguin, Landau, Verwey, and Overbeek (DLVO) [6, 7], repulsive electrostatic forces between charged colloids can stabilise a suspension against aggregation induced by van der Waals attractive forces [8].

Dispersed in a polar solvent, colloidal particles can acquire charge through dissociation of ionizable chemical groups at the surface. Electrostatic interactions are sensitive to the surface charges of the macroions and to the distribution of surrounding counterions. A macroion's bare (structural) charge depends on its surface chemistry (e.g., number and type of ionizable sites) and, in general, on the pH and salinity of the solution [9, 10]. Dressed by an entourage of strongly attracted counterions, a highly charged macroion can act as though carrying a significantly reduced (renormalized) *effective* charge.

The basic concepts of charge renormalization and effective charge were first introduced and widely explored some four decades ago in the context of polyelectrolyte solutions [11, 12]. Similar ideas were subsequently applied to colloidal suspensions by Alexander *et al.* [13], who demonstrated that strong association of counterions can significantly renormalize spherical macroion charges. Numerous experimental studies of deionized aqueous suspensions of highly charged spherical latex particles [14, 15, 16, 17], integral-equation calculations [18], and simulation studies of the primitive model [19, 20, 21, 22, 23] have since confirmed the effective charge as a physically important parameter in the one-component model of colloidal suspensions.

The one-component model provides a practical approach to overcoming the severe challenges of extreme size and charge asymmetries in explicit molecular models of charge-stabilised colloidal suspensions, polyelectrolyte solutions, and many other soft materials [24]. The model is derived from the multi-component ion mixture by averaging over the degrees of freedom of the microions (counterions and salt ions). The surviving "pseudo-macroions" are governed by effective electrostatic interactions, screened by the implicitly modeled microions.

This paper seeks to unite the concepts of dressed macroions and effective interactions in a coherent statistical mechanical framework that describes the association of counterions with macroions, the renormalization of the effective macroion charge, effective electrostatic interactions between macroions, and thermodynamic properties of deionized suspensions of highly charged colloids. Conceptually similar syntheses

have been proposed recently, based on Debye-Hückel theory [25, 26, 27, 28, 29] and on nonlinear Poisson-Boltzmann theory [30, 31]. The present theory is inspired by the elegant liquid-state approaches of Levin, Trizac, and coworkers [25, 26, 27, 28, 29], but differs in several significant practical respects.

The remainder of the paper is organized as follows. Sections 2 and 3 trace a path from the microscopic primitive model of charged colloids to an effective one-component model of dressed, charge-renormalized macroions. A simple criterion is adopted to differentiate between free and electrostatically bound counterions; physical approximations are developed for the free energies of the two counterion phases; and a variational method is prescribed for determining the renormalized effective charge and screening constant. Section 4 demonstrates the practical implementation of the theory and compares predictions for the pressure of deionized suspensions with corresponding data from both simulations of the primitive model and experiment. Excellent agreement is obtained, over broad ranges of system parameters, with trivial computational effort. Finally, Sec. 5 closes with a summary and perspectives.

2. Model

Within the primitive model of charged colloids, the macroions are modeled as negatively charged hard spheres of monodisperse radius a and bare valence Z_0 (charge $-Z_0e$), the microions as monovalent point charges, and the solvent as a dielectric continuum of uniform relative permittivity ϵ. Polarization effects and image charges are ignored, assuming index-matching of macroions and solvent. The suspension may be either entirely confined to a closed volume at fixed salt concentration or in partial chemical (Donnan) equilibrium (e.g., via a semi-permeable membrane) with a microion reservoir, which fixes the microion chemical potentials. The reservoir is presumed to be a 1:1 electrolyte solution with number density n_0 of monovalent salt ion pairs.

In the presence of a sufficiently strong attractive potential, some fraction of counterions may remain closely associated with the macroions. By analogy with Oosawa's two-phase theory of polyelectrolyte solutions [12], a distinction then can be drawn between free and bound microion regions ("phases"). In contrast to rodlike polyelectrolytes, however, spherical colloidal macroions do not generate a Coulomb potential of sufficient range to overcome counterion entropy and condense the counterions. As a result, associated counterions remain only thermally (not physically or chemically) bound to the macroions.

As Fig. 1 depicts, counterions localized within a spherical shell of thickness δ (yet to be determined) are regarded as renormalizing the bare macroion valence. Coions are assumed to be completely expelled from the shell. The resulting "dressed" macroion is a composite object consisting of a bare macroion and its shell of bound counterions with an effective valence $Z \leq Z_0$. Although the bare and effective valences are statistically fluctuating quantities, they are represented for present purposes by their average values.

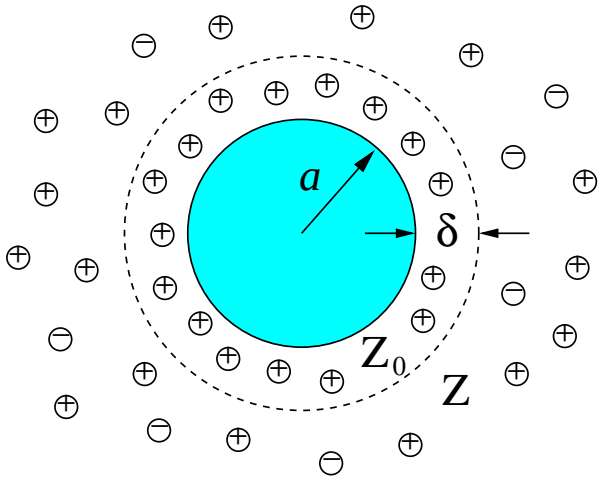

Figure 1. Model of charged colloidal suspension: spherical macroions of radius a and point microions dispersed in a dielectric continuum. Strongly associated counterions in a spherical shell of thickness δ renormalize the bare macroion valence Z_0 to an effective (lower) valence Z.

The boundary between free and bound counterions is located at a distance from the macroion surface at which the electrostatic energy of counterion-macroion attraction is comparable to the average thermal energy per counterion. Denoting by $\phi(r)$ the electrostatic potential at distance r from a macroion centre, the association shell is defined via

$$e|\phi(a+\delta)| = Ck_BT \ , \tag{1}$$

where C is an adjustable, dimensionless parameter, evidently of order unity. Counterions within the association shells ($a < r < a+\delta$) are assumed to be trapped in the potential wells of the macroions, while more distant counterions have sufficient kinetic (thermal) energy to escape. This simple criterion for δ justifies a Debye-Hückel-like linear-screening approximation for the free counterions, which is exploited in the theory developed below.

Previous studies have applied a thermal criterion similar to Eq. (1) to the electrostatic potential [32, 33, 34] or to the effective pair potential [35]. Alternative approaches to defining the association shell thickness are based on the structure of the counterions around a macroion or on the macroion configurations. Alexander *et al.* [13], for example, determined Z in a spherical cell model by matching the solutions of the nonlinear and linearized PB equations for the counterion density at the edge of the cell. The inflection point in the running effective charge of the macroion has been identified as another sensible boundary between free and bound counterions [36]. Yet another fruitful approach is to fit the effective one-component model (with a screened-Coulomb pair potential) to either the static structure factor measured in light-scattering experiments [14] or the pair distribution function computed in simulations of the primitive model [19, 20, 21, 22, 23]. A useful comparison of various criteria for defining effective charges is provided in ref. [34].

3. Theory

The theory proposed here for charge renormalization and thermodynamics of colloidal suspensions requires modeling the electrostatic potential and the total free energy of the system. For this purpose, the most popular framework is the Poisson-Boltzmann (PB) theory [37], a mean-field approach that is especially well-suited to suspensions with monovalent microions, whose correlations usually can be justifiably neglected. Combining the exact Poisson equation for the potential with a Boltzmann approximation for the microion density profiles (as functions of position $\mathbf{r}$), $n_\pm(\mathbf{r}) = n_0 \exp[\mp\psi(\mathbf{r})]$, the PB theory is based on the Poisson-Boltzmann equation

$$\nabla^2\psi = \kappa_0^2 \sinh\psi \ , \tag{2}$$

where $\psi = \beta e\phi$ is the reduced potential (vanishing in the reservoir), $\beta = 1/(k_B T)$ at temperature T, $\kappa_0 = \sqrt{8\pi\lambda_B n_0}$ is the Debye screening constant, and $\lambda_B = \beta e^2/\epsilon$ is the Bjerrum length. Equation (2) must be solved together with appropriate boundary conditions: $\nabla\psi|_{r=a} = Z_0\lambda_B/a^2$ and $\nabla\psi = 0$ either as $r \to \infty$ — far from the macroions in a bulk suspension — or at $r = R$ in a symmetric cell of radius R. Neglecting macroion-macroion correlations, and all but asymptotically long-range microion-microion correlations, the corresponding Helmholtz free energy takes the form

$$\beta F = \sum_{i=\pm} \int \mathrm{d}\mathbf{r}\, n_i(\mathbf{r})[\ln(n_i(\mathbf{r})\Lambda^3) - 1] + \frac{1}{8\pi\lambda_B}\int \mathrm{d}\mathbf{r}\, |\nabla\psi|^2 \ , \tag{3}$$

where Λ is the microion thermal de Broglie wavelength and the two terms on the right side represent, respectively, the ideal-gas free energy due to microion entropy and the total electrostatic energy.

At distances r for which $|\psi(r)| \ll 1$, the right side of Eq. (2) may be approximated by an expansion about the reservoir potential ($\psi = 0$) to linear order in ψ. Anticipating applications to deionized suspensions of highly charged colloids, however, the microion densities are here expanded instead about the mean (Donnan) potential of the suspension $\bar{\psi}$ [38, 39, 40]:

$$\nabla^2\psi = \kappa_0^2[\sinh\bar{\psi} + \cosh\bar{\psi}(\psi - \bar{\psi})] \ . \tag{4}$$

In a bulk suspension of macroions with bare valence Z_0, the solution of Eq. (4), with boundary condition $\psi'(r) \to 0$ as $r \to \infty$, yields the potential generated by a single bare macroion [41]:

$$\psi(r) = -Z_0\lambda_B \, \frac{e^{\kappa a}}{1+\kappa a} \, \frac{e^{-\kappa r}}{r} \ , \quad r \geq a \ , \tag{5}$$

with the bare screening constant

$$\kappa = \kappa_0\sqrt{\cosh\bar{\psi}} = \sqrt{4\pi\lambda_B(n_+ + n_-)} \ . \tag{6}$$

Here $n_\pm = n_0 \exp(\mp\bar{\psi}) = N_\pm/[V(1-\eta)]$ represent the mean number densities of microions in the *free* volume, i.e., the total volume V reduced by the fraction η occupied by the macroion hard cores. Note that the screening constant κ depends implicitly on the

average density of macroions, since the global constraint of electroneutrality relates the numbers of macroions (N_m) and microions ($N_\pm$) in the suspension via $Z_0 N_m = N_+ - N_-$. Combining the linearized PB equation [Eq. (4)] with a quadratic expansion of the ideal-gas free energy [Eq. (3)] about the mean microion densities yields the corresponding linear-screening approximation for the one-body part of the free energy per macroion:

$$\beta f = \sum_{i=\pm} x_i[\ln(n_i\Lambda^3) - 1] - \frac{Z_0^2}{2}\frac{\kappa\lambda_B}{1+\kappa a} - \frac{Z_0^2}{2}\,\frac{n_m}{n_+ + n_-}\ , \tag{7}$$

where $x_i = N_i/N_m$ and the three terms on the right side account for, respectively, the microion entropy, macroion self-energy, and the Donnan potential energy of the microions.

The PB theory proves to be formally equivalent to a class of effective-interaction theories that map the macroion-microion mixture onto a one-component model (OCM), by integrating over microion degrees of freedom in the partition function, and that neglect all but long-range microion correlations [24, 42]. The effective-interaction approach has been variously formulated as density-functional [43, 44, 45, 46, 47], extended Debye-Hückel [48], distribution-function [49, 50], and response [51, 52, 53, 54, 55] theories — all fundamentally equivalent [24], aside from technical differences in the incorporation of excluded-volume effects. The OCM is governed by an effective Hamiltonian comprising a one-body volume energy and summations over pair and, in general, many-body effective interactions.

Linearizing the PB equation about the mean potential [Eq. (4)], and the PB free energy about the mean microion densities, is completely equivalent in the OCM to linearizing the microion free energy about a reference system of neutral macroions embedded in an electroneutral microion plasma [42] and neglecting many-body effective interactions. Furthermore, the volume energy in the OCM turns out to be identical to the linearized PB free energy [Eq. (7)]. A significant advantage of the OCM, however, is its natural incorporation of effective interactions between macroions. An additional contribution to the total free energy then comes from the effective (reduced) macroion-macroion pair potential [52, 53]

$$\beta v_{\rm eff}(r) = Z_0^2\lambda_B\left(\frac{e^{\kappa a}}{1+\kappa a}\right)^2\frac{e^{-\kappa r}}{r}\ , \quad r > 2a\ . \tag{8}$$

Further progress requires uniting the OCM-based linear-screening theory of charged colloids with the charge renormalization model of Sec. 2. To this end, the total free energy is first separated, according to

$$F = F_{\rm free} + F_{\rm bound} + F_m\ , \tag{9}$$

into contributions from free and bound microions and from effective interactions between macroions, respectively. The linear-screening theory is then applied only to the free microions, whose free energy per macroion is approximated by [cf. Eq. (7)]

$$\beta f_{\rm free} = \sum_{i=\pm}\tilde{x}_i[\ln(\tilde{n}_i\Lambda^3) - 1] - \frac{Z^2}{2}\,\frac{\tilde{\kappa}\lambda_B}{1+\tilde{\kappa}(a+\delta)} - \frac{Z^2}{2}\,\frac{n_m}{\tilde{n}_+ + \tilde{n}_-}\ , \tag{10}$$

where $\tilde{x}_\pm = \tilde{N}_\pm/N_m$, $\tilde{N}_\pm$ are the numbers of free microions, $\tilde{n}_\pm = \tilde{N}_\pm/[V(1-\tilde{\eta})]$, and $\tilde{\eta} = \eta(1+\delta/a)^3$ is the effective volume fraction of the dressed macroions. Generalizing Eq. (5), the electrostatic potential around a dressed macroion of effective valence Z and effective radius $a+\delta$ is given by

$$\tilde{\psi}(r) = -Z\lambda_B \, \frac{e^{\tilde{\kappa}(a+\delta)}}{1+\tilde{\kappa}(a+\delta)} \, \frac{e^{-\tilde{\kappa}r}}{r}, \quad r \geq a+\delta \; , \tag{11}$$

with a renormalized screening constant

$$\tilde{\kappa} = \sqrt{4\pi\lambda_B(\tilde{n}_+ + \tilde{n}_-)} \; . \tag{12}$$

The association shell thickness is now specified by combining Eqs. (1) and (11), yielding

$$\frac{Z\lambda_B}{[1+\tilde{\kappa}(a+\delta)](a+\delta)} = C \; , \tag{13}$$

and solving self-consistently for δ (given Z), noting that $\tilde{\kappa}$ depends implicitly on δ.

The free energy of the bound counterions decomposes naturally into entropic and energetic contributions. The first contribution is the ideal-gas free energy of the bound counterions, given exactly by

$$\beta F_{\rm id} = 4\pi N_m \int_a^{a+\delta} {\rm d}r \, r^2 n_b(r) \left[\ln\left(n_b(r)\Lambda^3\right) - 1 \right] \; , \tag{14}$$

where $n_b(r)$ is the number density profile of bound counterions within the association shell and the integral covers the volume of the shell from inner radius a to outer radius $a+\delta$. Although $n_b(r)$ could be obtained by solving the nonlinear PB equation [Eq. (2)] (as in ref. [31]), the present study explores a simpler approximation, $\ln\left(n_b(r)\Lambda^3\right) \simeq \ln\left(n_b\Lambda^3\right)$, which yields

$$\beta F_{\rm id} \simeq N_m(Z_0 - Z) \left[\ln\left(n_b\Lambda^3\right) - 1 \right] \; , \tag{15}$$

where $n_b = (Z_0 - Z)/v_s$ is the mean density of bound counterions in the association shell of volume $v_s = (4\pi/3)[(a+\delta)^3 - a^3]$. The second contribution to the bound counterion free energy is the electrostatic energy $F_{\rm el}$ required to assemble the total charge of the dressed macroions — bare and bound charge — from infinity. An exact calculation would again require knowledge of the bound counterion density profile. Here we simply assume $n_b(r)$ to be sharply peaked near $r = a$ and take

$$\beta F_{\rm el} \simeq N_m \frac{Z^2\lambda_B}{2a} \; . \tag{16}$$

In the case of macroion charges below the renormalization threshold, $Z = Z_0$ and $F_{\rm el}$ is a trivial constant that is irrelevant for thermodynamics. At charges high enough that $Z < Z_0$, however, $F_{\rm el}$ becomes significant, since Z is state-dependent (as seen below). Combining Eqs. (15) and (16), the bound-counterion free energy per macroion is here simply approximated by

$$\beta f_{\rm bound} \simeq (Z_0 - Z) \left[\ln\left(\frac{Z_0 - Z}{v_s}\Lambda^3 \right) - 1 \right] + \frac{Z^2\lambda_B}{2a} \; . \tag{17}$$

For a given bare valence Z_0, the effective valence Z is prescribed by minimizing with respect to Z the total microion free energy [sum of Eqs. (10) and (17)] at fixed temperature and mean microion densities:

$$\left(\frac{\partial}{\partial Z}(f_{\rm free}+f_{\rm bound})\right)_{T,n_\pm}=0\ . \tag{18}$$

The same variational prescription has been adopted by Levin *et al.* [25, 26, 27]. It is easily shown that the minimization condition is equivalent to equating the chemical potentials of counterions in the free and bound phases, under the constraint that Z and δ are related by Eq. (13). The effective valence and corresponding shell thickness in turn determine the effective screening constant $\tilde{\kappa}$ via Eq. (12).

Once the effective valence and screening constant are determined, the effective pair potential between dressed macroions follows as

$$\beta\tilde{v}_{\rm eff}(r)=Z^2\lambda_B\left(\frac{e^{\tilde{\kappa}a}}{1+\tilde{\kappa}a}\right)^2\frac{e^{-\tilde{\kappa}r}}{r}\ ,\quad r>2(a+\delta)\ , \tag{19}$$

from which the macroion free energy F_m can be computed via liquid-state theory or computer simulation. (Note that the macroion radius is not renormalized in the prefactor of the effective pair potential in Eq. (19), since the association shells are penetrable.) For demonstration purposes, we implement a variational method [43, 55] based on first-order thermodynamic perturbation theory with a hard-sphere reference system [56]. The macroion free energy per macroion is thus approximated as

$$f_m(n_m,\tilde{n}_\pm)=\min_{(d)}\left\{f_{\rm HS}(n_m,\tilde{n}_\pm;d)+2\pi n_m\int_d^\infty {\rm d}r\, r^2 g_{\rm HS}(r,n_m;d)\tilde{v}_{\rm eff}(r,n_m,\tilde{n}_\pm)\right\}\ , \tag{20}$$

where the effective hard-sphere diameter d is the variational parameter and $f_{\rm HS}$ and $g_{\rm HS}$ are the excess free energy density and (radial) pair distribution function, respectively, of the HS fluid, computed here from the near-exact Carnahan-Starling and Verlet-Weis expressions [56]. Minimization of f_m with respect to d generates a least upper bound to the free energy. It is important, in practice, to fix the renormalized system parameters (Z, δ, $\tilde{\kappa}$) in this minimization and in all partial thermodynamic derivatives.

The thermodynamic pressure finally can be calculated from

$$p=n_m^2\left(\frac{\partial f}{\partial n_m}\right)_{T,N_s/N_m}=p_{\rm free}+p_m\ , \tag{21}$$

where $f=F/N_m$ is the total Helmholtz free energy per macroion, $N_s=N_-$ is the number of salt ion pairs in the suspension,

$$\beta p_{\rm free}=\tilde{n}_+ +\tilde{n}_- -\frac{Z(\tilde{n}_+-\tilde{n}_-)\tilde{\kappa}\lambda_B}{4[1+\tilde{\kappa}(a+\delta)]^2} \tag{22}$$

is the (reduced) pressure generated by the free microions, and

$$\beta p_m=n_m+n_m^2\beta\left(\frac{\partial f_m}{\partial n_m}\right)_{T,N_s/N_m} \tag{23}$$

is the macroion pressure due to macroion entropy and effective pair interactions. Note that, since Z and δ are implicitly held fixed in the partial derivatives, the bound

counterions make no contribution to the pressure. As an alternative to variational theory, computer simulation also can be used to determine the macroion pressure [57].

4. Results and Discussion

To demonstrate its implementation, the charge renormalization theory is now applied to deionized suspensions of charged colloids and monovalent microions in an aqueous solvent at room temperature ($\lambda_B = 0.72$ nm). As noted in Sec. 3, the theory involves a single free parameter, namely the dimensionless parameter C in Eq. (18), which establishes the threshold for charge renormalization. To ensure that a counterion's average thermal energy does not exceed its binding potential, C must be $\mathcal{O}(1)$. Lacking an independent, physical criterion, C must be regarded for the present as a fitting parameter. All results presented below were computed for $C = 3$, a value found to give satisfactory overall agreement with thermodynamic and structural data from primitive model simulations. In passing, we note that the thermal parameter C in the present theory is somewhat analogous to the adjustable cell radius parameter b in ref. [31], which combines PB cell and linear-screening theories.

The key physical concepts of the charge renormalization theory are illustrated in Figs. 2-4. For a sufficiently small bare valence, Eq. (13) admits no real solution for nonzero thickness of the association shell. In this case, there are no bound counterions ($\delta = 0$, $v_s = 0$) and the free energy is minimized by $Z = Z_0$ (dashed line in Fig. 2). At a threshold value of the bare valence, however, the shell emerges continuously and thickens rapidly with increasing Z_0 at fixed volume fraction and salt concentration (inset to Fig. 2), while the free energy minimum shifts to $Z < Z_0$ (solid curve in Fig. 2). The effective valence does not saturate, but continues to grow logarithmically with increasing Z_0, in contrast to the behaviour expected and observed for polyelectrolytes [12] and to predictions for colloidal suspensions from PB cell-based theories [13, 36, 30] and Debye-Hückel-based theories [25, 26, 27, 28, 29].

As Figs. 3 and 4 show, Z varies with volume fraction η and salt concentration c_s of the suspension. The effective valence thus depends nontrivially on the thermodynamic state, exhibiting a pronounced minimum with respect to η and increasing monotonically with c_s. Correspondingly, the association shell thins with increasing η and c_s (Figs. 3 and 4, insets), in such a manner, however, that the shells surrounding neighbouring macroions always remain separate and distinct. The absence of overlapping shells provides an internal consistency check on the theory.

To test predictions of the theory for thermodynamic properties, the pressures of deionized suspensions, calculated from Eqs. (12), (13), and (21)-(23), are directly compared with available data from simulations of the primitive model. Figures 5 and 6 show comparisons with the results of Linse [21] from extensive Monte Carlo simulations of salt-free suspensions with various bare valences and electrostatic coupling parameters $\Gamma = \lambda_B/a$. The unrenormalized linear-screening theory [52, 53] performs excellently for low-to-moderate couplings ($\Gamma < 0.1779$ for $Z_0 = 40$ in Fig. 5), but breaks down at

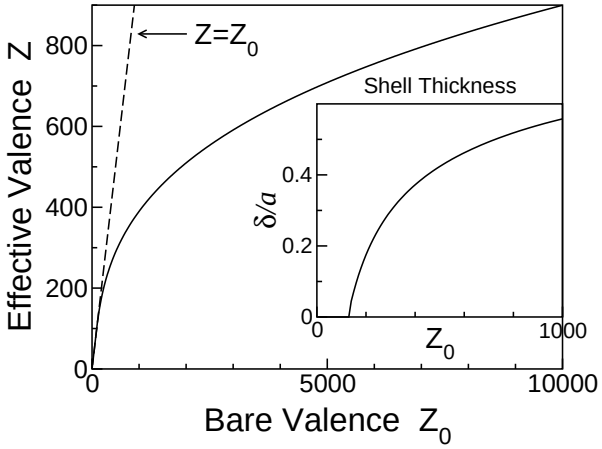

Figure 2. Effective valence Z vs. bare valence Z_0 for a deionized suspension ($c_s \simeq 0$) of macroions of radius $a = 50$ nm and volume fraction $\eta = 0.1$. Inset: counterion association shell emerges and thickens beyond threshold Z_0.

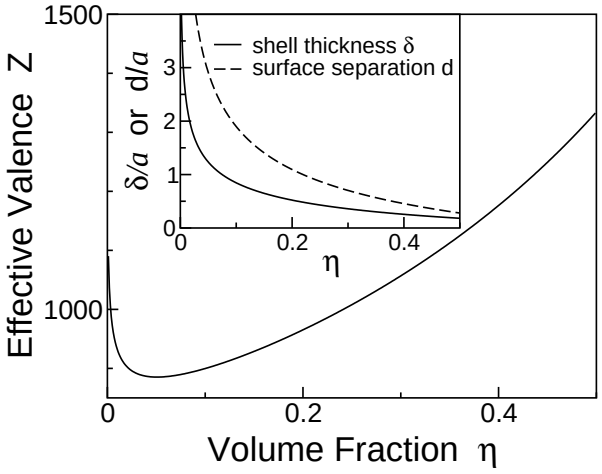

Figure 3. Effective valence Z vs. volume fraction η for a deionized suspension of macroions of radius $a = 50$ nm and bare valence $Z_0 = 10^4$. Inset: association shell (solid curve) thins with increasing η, remaining thinner than nearest-neighbour surface separation in fcc crystal (dashed curve).

higher couplings, characteristic of highly charged latex particles and ionic surfactant micelles. As illustrated in Figs. 5(b) and 6 (inset), charge renormalization becomes important for $Z_0\Gamma > 7$, where the effective valence tends to be lower than the bare valence. The renormalized theory restores close agreement with simulation up to at least $Z_0\Gamma \simeq 28$ ($\Gamma = 0.7115$ in Fig. 5). In practice, the excluded-volume correction to the microion densities in Eq. (10), and the inclusion of the effective pair pressure — already important features of the unrenormalized theory [57] — are essential for consistent quantitative accuracy as the volume fraction becomes renormalized. Remarkably and intriguingly, the threshold for charge renormalization coincides with the onset of a spinodal phase instability, at low but non-zero salt concentrations, predicted by linear-

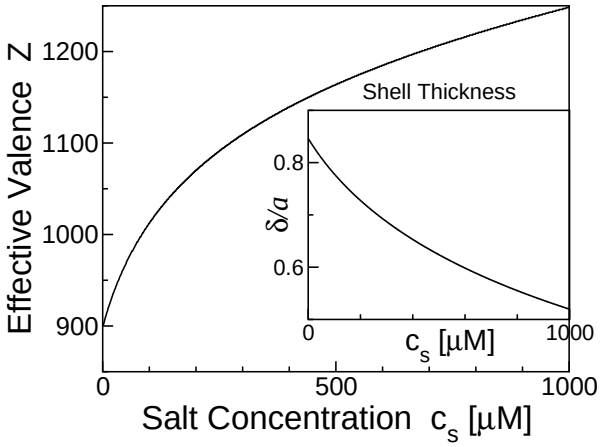

Figure 4. Effective valence Z vs. system salt concentration c_s for macroions of radius $a = 50$ nm, bare valence $Z_0 = 10^4$, and volume fraction $n = 0.1$. Inset: association

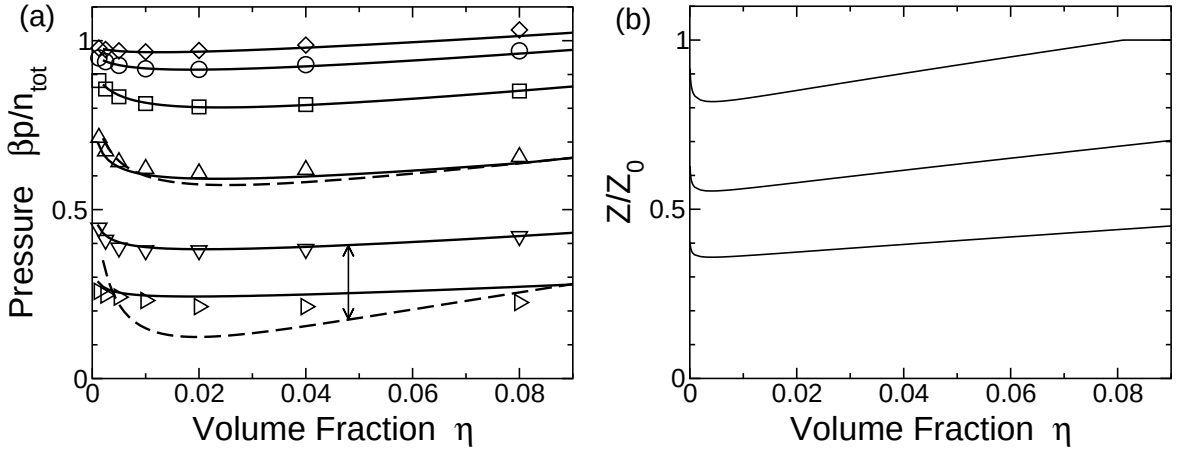

Figure 5. (a) Total reduced pressure $\beta p/n_{\rm tot}$ vs. macroion volume fraction η, where $n_{\rm tot} = (Z_0 + 1)n_m$ (total ion density), of salt-free suspensions with bare macroion valence $Z_0 = 40$ and electrostatic coupling constants (top to bottom) $\Gamma = 0.0222$, 0.0445, 0.0889, 0.1779, 0.3558, 0.7115. Symbols: Monte Carlo simulations of the primitive model [21] (symbol sizes exceed error bars). Curves: variational theory with (solid) and without (dashed) charge renormalization. The double-ended arrow points to corresponding curves for $\Gamma = 0.3558$. The dashed curve for $\Gamma = 0.7115$ is off-scale, the pressure being negative. (b) Corresponding ratio of effective to bare macroion valence Z/Z_0 vs. η for $\Gamma = 0.1779$, 0.3558, 0.7115 (top to bottom). For $\Gamma \leq 0.1$, no renormalization is predicted ($Z = Z_0$).

screening theories [43, 45, 48, 55]. This rather unusual prediction, however, has not yet been confirmed by primitive model simulations and the experimental situation is unresolved.

Finally, the theory also can be tested against available experimental data. Figure 7 shows a comparison of predictions with osmotic pressure measurements of deionized, aqueous, charged colloidal crystals reported by Reus *et al.* [58]. Since bare (titratable)

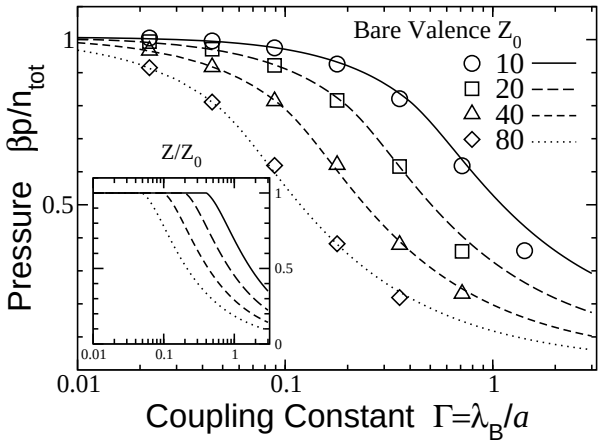

Figure 6. Total reduced pressure $\beta p/n_{\rm tot}$ vs. electrostatic coupling constant Γ of salt-free suspensions with fixed volume fraction $\eta = 0.01$ and bare macroion valence (top to bottom) $Z_0 = 10, 20, 40, 80$. Open symbols: Monte Carlo simulations of the primitive model [21] (symbol sizes exceed error bars). Curves: charge-renormalized variational theory. Inset: Ratio of effective to bare macroion valence Z/Z_0 vs. Γ.

charges are notoriously difficult to characterize in experiments, Z_0 is treated here as a fitting parameter, a value of $Z_0 \simeq 3000$ giving a reasonable fit to the data. As seen in the inset to Fig. 7, the effective charge in this case is substantially lower than the bare charge. It is important to emphasize, however, that only thermodynamic quantities have physical significance within the theory and that the theoretically defined variable Z does not necessarily correspond directly with any effective charge that may be determined experimentally, e.g., by light scattering, electrophoresis, or conductivity measurements. Moreover, direct comparisons between theory and experiment are subject to complication by charge regulation via chemical reactions at the macroion surface [9, 10], which may render even the bare charge dependent on thermodynamic state, e.g., pH and salinity.

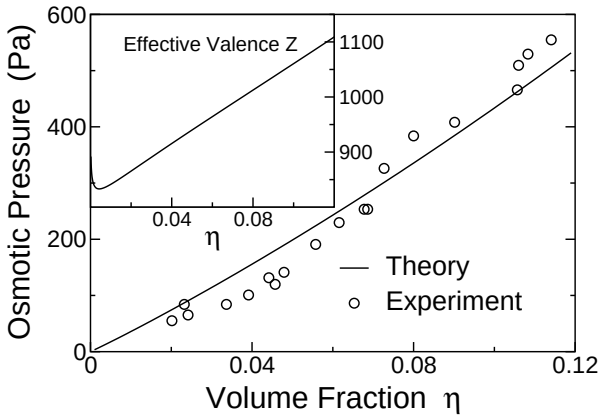

Figure 7. Osmotic pressure (in Pa units) vs. volume fraction η for a deionized suspension ($c_s = 0$) of charged macroions of radius $a = 51$ nm and bare valence $Z_0 = 3000$. Curve: charge renormalization theory; symbols: experimental data [58]. Inset: effective valence Z vs. η.

5. Conclusions

In summary, a new theory of charge renormalization in charge-stabilised colloidal suspensions has been developed and implemented. The theory posits the existence of free and bound counterion phases and integrates a thermal criterion for distinguishing between the two phases with an effective-interaction theory based on a one-component model. Within the theory, bound counterions act to renormalize the effective valence of the dressed macroions, while free counterions screen the dressed macroions and make the dominant contribution to the pressure. A linear-screening approximation accurately describes monovalent free counterions, while the bound counterions are adequately described by a comparatively crude coarse-grained approximation for the bound-counterion density profile.

Despite the conceptual and practical simplicity of the charge renormalization theory, predictions for the pressure closely agree with corresponding data from both primitive model simulations and an experiment, over ranges of macroion charges, volume fractions, and electrostatic coupling strengths, demonstrating the practical potential of the theory for modeling equilibrium thermodynamic properties. A preliminary simulation study [59] indicates that the theory also can accurately model structural properties, such as macroion-macroion pair distribution functions, although within a more limited range of electrostatic couplings. Future work will focus on refinements of the theory, further comparisons with experiment, and applications to the phase behaviour of deionized suspensions of highly charged macroions in bulk and in confinement [60, 61, 62].

Acknowledgments

This work was supported by the National Science Foundation (DMR-0204020) and the Petroleum Research Fund (PRF 44365-AC7). Fruitful discussions with Ben Lu and helpful correspondence with Per Linse are gratefully acknowledged.

[1] D. F. Evans and H. Wennerström, *The Colloidal Domain* (2nd ed.) (Wiley-VCH, New York, 1999).
[2] K. S. Schmitz, *Macroions in Solution and Colloidal Suspension* (VCH, New York, 1993).
[3] J. Israelachvili, *Intermolecular and Surface Forces* (Academic, London, 1992).
[4] C. M. Soukoulis, *Photonic Band Gap Materials* (Kluwer, Dordrecht, 1996).
[5] J. E. G. J. Wijnhoven and W. L. Vos, *Science* **281**, 802 (1998).
[6] B. V. Derjaguin and L. Landau, Acta Physicochimica (URSS) **14**, 633 (1941).
[7] E. J. W. Verwey and J. T. G. Overbeek, *Theory of the Stability of Lyophobic Colloids* (Elsevier, Amsterdam, 1948).
[8] For reviews of colloidal interactions, see C. N. Likos, Phys. Rep. **348**, 267 (2001); L. Belloni, *J. Phys.: Condens. Matter* **12**, R549 (2000); J. P. Hansen and H. Löwen, Annu. Rev. Phys. Chem. **51**, 209 (2000).
[9] O. Spalla and L. Belloni, *J. Chem. Phys.* **95**, 7689 (1991).
[10] H. H. von Grünberg, J. Coll. Int. Sci. **219**, 339 (1999).
[11] G. S. Manning, *J. Chem. Phys.* **51**, 924 (1969).
[12] F. Oosawa, *Polyelectrolytes* (Dekker, New York, 1971).
[13] S. Alexander, P. M. Chaikin, P. Grant, G. J. Morales, and P. Pincus, *J. Chem. Phys.* **80**, 5776 (1984).
[14] T. Gisler, S. F. Schulz, M. Borkovec, H. Sticher, P. Schurtenberger, B. D'Aguanno, and R. Klein, *J. Chem. Phys.* **101**, 9924 (1994).
[15] T. Palberg, W. Mönch, F. Bitzer, R. Piazza, and T. Bellini, *Phys. Rev. Lett.* **74**, 4555 (1995).
[16] P. Wette, H. J. Schöpe, and T. Palberg, *J. Chem. Phys.* **116**, 10981 (2002).
[17] D. G. Grier, *J. Phys.: Condens. Matter* **12**, A85 (2000).
[18] L. Belloni, *J. Chem. Phys.* **85**, 519 (1986).
[19] M. J. Stevens, M. L. Falk, and M. O. Robbins, *J. Chem. Phys.* **104**, 5209 (1996).
[20] P. Linse and V. Lobaskin, *Phys. Rev. Lett.* **83**, 4208 (1999).
[21] P. Linse, *J. Chem. Phys.* **113**, 4359 (2000). Reduced pressures in Table III of this paper should be $\beta p/n_{\rm tot} = 0.361$ for $Z = 10$, $\Gamma = 1.423$, $\eta = 0.01$; 0.970 for $Z = 40$, $\Gamma = 0.0222$, $\eta = 0.005$; and 0.971 for $Z = 40$, $\Gamma = 0.0222$, $\eta = 0.02$ (P. Linse, private communication).
[22] V. Lobaskin, A. Lyubartsev, and P. Linse, *Phys. Rev.* E **63**, 020401(R) (2001).
[23] V. Lobaskin and K. Qamhieh, *J. Phys. C: Solid State Phys.* B **107**, 8022 (2003).
[24] A. R. Denton, in *Nanostructured Soft Matter: Experiment, Theory, Simulation and Perspectives*, ed. A. V. Zvelindovsky (Springer, Dordrecht, 2007).
[25] Y. Levin, M. C. Barbosa, and M. N. Tamashiro, Europhys. Lett. **41**, 123 (1998).
[26] M. N. Tamashiro, Y. Levin, and M. C. Barbosa, Eur. Phys. J. B **1**, 337 (1998).
[27] A. Diehl, M. C. Barbosa, and Y. Levin, Europhys. Lett. **53**, 86 (2001).
[28] Y. Levin, E. Trizac, and L. Bocquet, *J. Phys.: Condens. Matter* **15**, S3523 (2003).
[29] E. Trizac and Y. Levin, *Phys. Rev.* E **69**, 031403 (2004).
[30] L. Bocquet, E. Trizac, and M. Aubouy, *J. Chem. Phys.* **117**, 8138 (2002).
[31] B. Zoetekouw and R. van Roij, *Phys. Rev. Lett.* **97**, 258302 (2006).
[32] K. S. Schmitz, Langmuir **15**, 4093 (1999).
[33] V. Sanghiran and K. S. Schmitz, Langmuir **16**, 7566 (2000).
[34] A. K. Mukherjee, K. S. Schmitz, and L. B. Bhuiyan, Langmuir **18**, 4210 (2002).
[35] D. B. Lukatsky and S. A. Safran, *Phys. Rev.* E **63**, 011405 (2000).

[36] L. Belloni, Colloids Surf. A **140**, 227 (1998).
[37] M. Deserno and C. Holm, in *Electrostatic Effects in Soft Matter and Biophysics*, vol. 46, NATO Advanced Studies Institute, Series II: Mathematics, Physics and Chemistry, edited by C. Holm *et al.* (Kluwer, Dordrecht, 2001).
[38] R. Klein and H. H. von Grünberg, Pure Appl. Chem. **73**, 1705 (2001).
[39] M. Deserno and H. H. von Grünberg, *Phys. Rev.* E **66**, 011401 (2002).
[40] M. N. Tamashiro and H. Schiessel, *J. Chem. Phys.* **119**, 1855 (2003).
[41] In the PB cell model [38, 39, 40], the cell boundary conditions modify the form of the electrostatic potential compared with Eq. (5).
[42] A. R. Denton, *Phys. Rev.* E **76**, 051401 (2007).
[43] R. van Roij and J.-P. Hansen, *Phys. Rev. Lett.* **79**, 3082 (1997).
[44] H. Graf and H. Löwen, *Phys. Rev.* E **57**, 5744 (1998).
[45] R. van Roij, M. Dijkstra, and J.-P. Hansen, *Phys. Rev.* E **59**, 2010 (1999).
[46] R. van Roij and R. Evans, *J. Phys.: Condens. Matter* **11**, 10047 (1999).
[47] B. Zoetekouw and R. van Roij, *Phys. Rev.* E **73**, 21403 (2006).
[48] P. B. Warren, *J. Chem. Phys.* **112**, 4683 (2000); *J. Phys.: Condens. Matter* **15**, S3467 (2003); *Phys. Rev.* E **73**, 011411 (2006).
[49] B. Beresford-Smith, D. Y. C. Chan, and D. J. Mitchell, J. Coll. Int. Sci. **105**, 216 (1985).
[50] D. Y. C. Chan, P. Linse, and S. N. Petris, Langmuir **17**, 4202 (2001).
[51] M. J. Grimson and M. Silbert, Mol. Phys. **74**, 397 (1991).
[52] A. R. Denton, *J. Phys.: Condens. Matter* **11**, 10061 (1999).
[53] A. R. Denton, *Phys. Rev.* E **62**, 3855 (2000).
[54] A. R. Denton, *Phys. Rev.* E **70**, 31404 (2004).
[55] A. R. Denton, *Phys. Rev.* E **73**, 41407 (2006).
[56] J.-P. Hansen and I. R. McDonald, *Theory of Simple Liquids*, 2^{nd} edition (Academic, London, 1986).
[57] B. Lu and A. R. Denton, *Phys. Rev.* E **75**, 061403 (2007).
[58] V. Reus, L. Belloni, Th. Zemb, N. Lutterbach, and H. Versmold, Journal de Physique II **7**, 603 (1997).
[59] B. Lu and A. R. Denton, unpublished.
[60] D. Frydel, S. Dietrich, and M. Oettel, *Phys. Rev. Lett.* **99**, 118302 (2007).
[61] J. Zwannikken and R. van Roij, *Phys. Rev. Lett.* **99**, 178301 (2007).
[62] S. H. L. Klapp, Y. Zeng, D. Qu, and R. von Klitzing, *Phys. Rev. Lett.* **100**, 118303 (2008). Note that the electrostatic coupling strength considered in these experiments and simulations ($Z_0 = 35$, $a = 13$ nm: $Z_0\Gamma < 2$) lies far below the predicted threshold for charge renormalization ($Z_0\Gamma \simeq 7$).